

# Spinning Speed–Throughput Rate Relationships for Polyester, Nylon, and Polypropylene Fibers

V. B. GUPTA, S. A. MONDAL, Y. C. BHUVANESH\*

Department of Textile Technology, Indian Institute of Technology, New Delhi 110 016, India

Received 29 June 1996; accepted 22 January 1997

**ABSTRACT:** The relationship between spinning speed and throughput rate has been investigated for fibers having the same fiber denier in the drawn state when produced by melt spinning of poly(ethylene terephthalate), nylon 6, and polypropylene polymers over a range of take-up speed (750–3000 m min<sup>-1</sup>) and throughput rate. To understand the structural origin of the relationship, a limited amount of characterization of structure and properties of the as-spun and drawn fibers was also done. A comparison of the results for the three polymers shows that while the increase in productivity with increase in spinning speed is relatively less for polyester and nylon 6, it is quite high for polypropylene. The birefringence data show that while molecular orientation increases rapidly with increasing wind-up speed in polyester and nylon 6, the rate of increase is relatively less in the case of polypropylene. The possible reasons for the observed differences in behavior are discussed. © 1997 John Wiley & Sons, Inc. *J Appl Polym Sci* **65**: 1773–1788, 1997

**Key words:** melt spinning; nylon 6; poly(ethylene terephthalate); polypropylene; productivity; spinning speed; throughput rate

## INTRODUCTION

An increase in productivity during melt spinning of thermoplastic polymers through the use of higher production speeds or by an increase in throughput rates with the basic aim of producing a yarn of specified drawn denier and textile grade properties is an important industrial goal. Production of melt-spun fibers at high spinning speeds (3000–4000 m min<sup>-1</sup>) offers benefits like improved productivity of the melt spinning process and in some cases better storage stability of the as-spun yarns. In general, the limiting spinning speed is decided through an optimization of the benefits offered by high spinning speeds. Riggert<sup>1</sup> found the optimum spinning speed in the

case of poly(ethylene terephthalate) (PET) to be ~ 3000–3500 m min<sup>-1</sup> and ~ 4000–4500 m min<sup>-1</sup> for nylon 6 (N6), depending on the drawn fiber deniers to be produced. Quite expectedly, the optimum spinning speed was higher for producing heavier deniers. Beyond these optimum speeds, gain in productivity drops rapidly with increase in spinning speed. This is perhaps a consequence of the growing orientation in the spun yarn. Filaments of superior molecular orientation need a lower draw ratio in the subsequent drawing procedure. This means that the denier of the undrawn filaments must be lowered in order to maintain the denier of the drawn yarn constant. Riggert proposed the following relationship<sup>1</sup>:

$$W = (\lambda \times V_L \times \text{den})/9000 \quad (1)$$

where  $W$  is the mass throughput rate (g min<sup>-1</sup>),  $\lambda$  is the effective draw ratio,  $V_L$  is the spinning speed (m min<sup>-1</sup>), and den is the final denier of

Correspondence to: V. B. Gupta.

\* Present address: School Of Textiles & Polymer Science, Clemson University, Clemson, SC 29634.

© 1997 John Wiley & Sons, Inc. CCC 0021-8995/97/091773-16

the drawn yarn. Two points are worth noting. First that

$$\lambda \times \text{den} = \text{spun denier} \quad (2)$$

and second that the extent of orientation or residual draw ratio would be different for fibers spun from different polymers at a particular speed. It is interesting to point out that eq. (1) can be shown to be equivalent to the continuity equation used in melt spinning, which applies to the entire spinline and takes the following form at the wind-up:

$$W = (A_L \times V_L \times \rho_L) \quad (3)$$

where  $A_L$  and  $\rho_L$  are, respectively, the cross-sectional area and density of the spun filament at the wind-up.

To gain an insight into the role of various process conditions that affect productivity for different polymers, a study was undertaken by melt-spinning samples from PET, N6, and polypropylene (PP) by varying spinning speeds and throughput rates to obtain drawn fibers with specified constant denier. Two points are worth making at this stage. First, it needs to be emphasized that the choice of throughput rate for a given spinning speed will be limited by such constraints. Second, an in-depth understanding of the overall interactions between processing conditions and structure development, more specifically orientation in the spun yarn, will require a much more detailed study than the present one. However, some aspects of this important subject have been considered in this investigation; for example, by comparing some of our data with those of other authors, the roles of some other processing parameters, like spinning temperature and molecular weight, have been considered in this paper.

The three polymers, PET, N6, and PP, were selected so that the roles played by differences in crystallinity and crystallization rates could be explored, as an understanding of these factors is crucial in arriving at the processing conditions that best suit each polymer or in exploring possibilities of improving production rates. PET does not undergo any crystallization in the range of spinning speeds investigated (up to 3000 m min<sup>-1</sup>) and produces largely amorphous spun yarns. After prolonged room conditioning, it crystallizes by a small amount. To develop crystallinity, drawing or annealing is required. In the case

of N6, the onset of stress-induced crystallization takes place<sup>2</sup> at spinning speeds of 2000–3000 m min<sup>-1</sup>. However, due to the role of moisture in lowering the glass transition temperature, the as-spun N6 yarns undergo significant structural changes and develop crystallinity on the bobbin<sup>3–5</sup> after very short periods of room conditioning. The conditioned as-spun yarns are almost always crystalline. Melt spinning of PP yarns invariably produces yarns with a relatively high degree of crystallinity. PP crystallizes in the spinline itself due to its higher rate of crystallization.

It was quite obvious at the start of the investigation that improvement in productivity is also related to the orientation and overall structure developed in the as-spun yarns. Hence, the structural features of the as-spun yarns were investigated and their salient features are also discussed in this article. Thermal analysis of the as-spun yarns was also carried out and is discussed in some detail. Some mechanical properties have also been studied.

## EXPERIMENTAL

### Sample Preparation

Fiber-grade PET chips were supplied by Indian Organic Chemicals Ltd., India. The polymer chips were dried in a vacuum oven at a temperature of 140°C for 16–18 h and then transferred to a hopper that was later purged with dry nitrogen, before the spinning operation. This operation was sufficient to attain a moisture content < 0.004% by weight. Fiber-grade N6 chips were supplied by LML Ltd., India. N6 chips were also subjected to a drying operation in a vacuum oven at 130°C for 16–18 h. PP chips (polymer-grade VS 6500H) of melt flow index 20 were obtained from Shell Company. No predrying was necessary for the PP chips.

### Melt Spinning

Melt spinning was carried out on a pilot scale Fourne Melt Spin Tester (SST-1207) with two spinnerets containing 26 holes each. The diameter of each capillary hole was 0.3 mm with an aspect ratio (L/D ratio) of 2. Four spinning speeds were used with each polymer, 750, 1500, 2250, and 3000 m min<sup>-1</sup>, to produce multifilament yarns. All other spinning conditions for any particular polymer were kept identical except the throughput rate, which was varied with spinning speed

**Table I Melt Spinning Conditions**

Sample	Spinning Speed (m/min)	Spinning Temp. (°C)	Metering Pump (rpm)	Throughput Rate (g/min)	Denier per Filament
PET					
P750	750	289	10.5	14.75	3.11
P1500	1500	289	18.0	25.27	2.75
P2250	2250	289	22.7	31.87	2.40
P3000	3000	289	28.0	39.39	2.00
N6					
N750	750	285	13.0	14.97	3.45
N1500	1500	285	21.0	24.20	2.80
N2250	2250	285	23.0	26.50	2.04
N3000	3000	285	25.0	28.80	1.66
PP					
PP750	750	260	16.0	13.6	3.14
PP1500	1500	260	28.0	24.4	2.81
PP2250	2250	260	39.0	34.6	2.66
PP3000	3000	260	50.5	44.5	2.56

on the basis of previous experience with the specific aim of obtaining fully drawn textile grade 60/52 multifilament yarns, i.e., yarns of  $\sim 60$  denier and 52 filaments. The temperature of spinning for each polymer was maintained constant at all spinning speeds and was chosen based on previous experience. In the case of N6 and PP, the first attempt did not yield drawn yarns of the required denier. Hence, slight adjustments were made in the throughput rate and a second set of spun yarns was obtained. The adjustments in throughput rates for the second set of spun samples were made on the basis of eq. (1) by considering the residual draw ratio of the first set of spun yarns so that the second set of spun yarns would yield drawn yarns of the requisite denier. The melt spinning parameters used are tabulated in Table I. The structural characteristics for the as-spun samples of N6 and PP were obtained only for the first set of samples; however, since the differences between the first and second set of samples are not very large, it will be assumed that the data will be applicable to the second set of samples also.

### Drawing

As-spun yarns were drawn on a laboratory model two-stage drawing machine to an appropriate draw ratio which was taken to be equal to (breaking elongation percentage - 30 percent); the breaking elongation being obtained from a load-elongation curve. This procedure allowed  $\sim 30\%$

of residual draw to remain in the drawn yarns. If the as-spun yarn did not yield a 60/52 multifilament drawn yarn and the required textile grade properties, a fresh set of as-spun yarns was obtained to fulfill the above set of requirements. The final set of drawn yarns obtained was characterized for some structural and mechanical characteristics. This was done to determine whether the properties of a set of samples prepared from a particular polymer were close to each other. The conditions used for drawing the various samples to arrive at the first set of drawn yarns are given in Table II. The most appropriate temperature of drawing for each polymer was also chosen based on previous experience.

### Physical and Structural Characterization of As-Spun and Drawn Yarns

#### Measurement of Denier

The deniers of the as-spun and drawn yarns were estimated by preparing skeins of 120 yard length of yarn on a wrap roll and weighing it accurately with the help of a sensitive electronic balance. The denier values reported are the average of measurements carried out on five samples prepared from each yarn.

#### Density

The sample densities were measured using a Davenport density gradient column. The liquids used

**Table II Drawing Conditions**

Sample	First Stage Drawing		Second Stage Drawing		Total Draw Ratio
	Draw Ratio	Draw Temp. (°C)	Draw Ratio	Draw Temp. (°C)	
P750	1.30	90	2.31	160	3.0
P1500	1.30	90	1.95	160	2.55
P2250	1.30	90	1.60	160	2.10
P3000	1.30	90	1.43	160	1.75
N750	1.31	r.t.*	2.22	50	2.90
N1500	1.22	r.t.	1.92	50	2.35
N2250	1.22	r.t.	1.43	50	1.75
N3000	1.14	r.t.	1.22	50	1.40
PP750	1.31	r.t.	2.18	130	2.85
PP1500	1.31	r.t.	1.87	130	2.45
PP2250	1.31	r.t.	1.78	130	2.33
PP3000	1.22	r.t.	1.87	130	2.28

\* r.t. indicates room temperature.

in preparing the liquid column for measuring the density of the as-spun and drawn yarns were carbon tetrachloride and *n*-heptane for PET and N6, and isopropanol and diethylene glycol for PP.

### Density Crystallinity

The volume fraction crystallinities of the as-spun and drawn yarns ( $\beta_d$ ) were estimated from the densities of the samples by using the following expression

$$\beta_d = \frac{\rho - \rho_{am}}{\rho_c - \rho_{am}} \quad (4)$$

where  $\rho$ ,  $\rho_{am}$ , and  $\rho_c$  are the densities of the sample, the standard amorphous, and standard crystalline phase, respectively. The values of  $\rho_{am}$  and  $\rho_c$  for the three polymers are given in Table III.

**Table III Standard Amorphous and Crystal Densities Used in Calculating Density Crystallinity for Various Polymers**

Polymer	$\rho_{am}$ (g/cm <sup>3</sup> )	$\rho_c$ (g/cm <sup>3</sup> )
PET (Ref. 6)	1.335	1.455
N6 (Ref. 7)	1.11	1.23
PP (Ref. 8)	0.854	0.946

### Birefringence ( $\Delta n$ )

The birefringence measurements on the as-spun and drawn yarns were made on a polarizing microscope fitted with a tilting compensator.

### X-ray Studies

X-ray diffractograms were recorded for the as-spun and drawn yarns in the form of finely cut pieces, almost like a powder, on a Phillips x-ray generator using Cu-K $\alpha$  radiation. The sample was scanned at the rate of 2° min<sup>-1</sup> from  $2\theta = 10$ –40° for PET and from  $2\theta = 10$ –35° for the N6 and PP samples. The X-ray intensity scans allowed an estimate of the crystalline fraction to be made (as described below) and also provided additional useful information on the various polymorphic states present in the crystalline part of the samples.

Farrow and Preston's method<sup>9</sup> was used to evaluate the crystallinity of the samples. The amorphous standards for PET and N6 were prepared in the laboratory, while the amorphous standard curve for PP was taken from the literature.<sup>10</sup> The scattered X-ray intensity from the amorphous standard was fitted below the X-ray intensity curve of the sample in each case after appropriate normalization. The degree of X-ray crystallinity ( $\beta_x$ ) was estimated from the area under the curve due to the crystalline portion as a fraction of the total area.

### Differential Scanning Calorimetry (DSC)

DSC studies were carried out on a Perkin-Elmer differential scanning calorimeter DSC 7 for the as-spun and drawn yarns which were first cut into thin pieces and then dried. Seven mg of this sample was then scanned at heating and cooling rates of  $10^{\circ}\text{C min}^{-1}$  in the temperature range of 50–300°C for the PET samples, 50–250°C for N6 samples, and 50–200°C for PP samples in nitrogen atmosphere. In addition to obtaining information on the crystallization and melting, DSC crystallinity,  $\beta_{\text{DSC}}$ , was obtained from the DSC scans using the following equation

$$\beta_{\text{DSC}} = \Delta H_f / \Delta H_f^{\circ} \quad (5)$$

where  $\Delta H_f$  is the heat of fusion obtained from the melting endotherm, and  $\Delta H_f^{\circ}$  is the heat of fusion of the standard crystalline sample which was taken from the literature.

### Tensile Properties

Load-elongation characteristics of the as-spun and drawn yarns at room temperature were obtained with the help of an Instron tensile tester (model 4202) using samples of 100 mm length and an extension rate of  $100 \text{ mm min}^{-1}$ .

In the case of as-spun PP yarn, load-extension behavior was also studied at  $130 \pm 1^{\circ}\text{C}$  on another Instron tensile tester (model 1112) fitted with an environmental chamber. Samples of gauge length 50 mm and an extension rate of  $100 \text{ mm min}^{-1}$  were used. The high-temperature tensile tests were carried out to examine the efficacy of the residual draw based on the high-temperature extensibility ( $130^{\circ}\text{C}$ ) of PP to arrive at an appropriate draw ratio. However, it was found that the draw ratio determined on the basis of the room temperature residual draw was more realistic, since all the drawn yarns obtained by using this draw ratio were closer to having the required textile-grade properties.

## RESULTS AND DISCUSSION

### Structural Characteristics of As-Spun Yarns

The physical and structural characteristics of the as-spun yarns are summarized in Table IV and will now be briefly discussed.

### Poly(ethylene terephthalate)

It may be clearly seen from Table IV that both the density and birefringence (orientation) of the PET yarns spun at higher speeds are greater. The samples are almost entirely amorphous, as suggested by the X-ray crystallinity for the samples spun at 2250 and  $3000 \text{ m min}^{-1}$ , whose powder diffractograms are shown in Figure 1.

### Nylon 6

Like PET yarns, N6 yarns (Table IV), spun at higher speeds generally show higher density and birefringence. It may be worth mentioning that the data obtained for the N6 as-spun yarns include the effects of crystallization and other structural changes that occur upon storage.<sup>3–5</sup> The X-ray powder diffractograms for the as-spun yarns (Fig. 2) show the presence of the  $\alpha$ - ( $2\theta = 21.5^{\circ}$ ) and  $\gamma$ - ( $2\theta = 23.3^{\circ}$ ) forms. Heuvel and Huisman<sup>2</sup> report that the as-spun and conditioned N6 yarns show various amounts of the  $\alpha$  and  $\gamma$  crystalline modifications. Although the unit cells of both crystal forms are monoclinic, the  $\alpha$ -crystal form shows an extended zig-zag conformation with the hydrogen bonds connecting antiparallel chains.<sup>11</sup> According to Arimoto,<sup>12</sup> the  $\gamma$ -form is similar to the  $\alpha$ -form in the basal plane except that the hydrogen bonds connect parallel molecules, which forces the chains to twist slightly to realize this conformation. These factors are also likely to influence the properties of the as-spun yarns. However, no attempt was made to take into account these factors.

### PP

The density of the as-spun PP yarns (Table IV) can also be seen to increase with spinning speed except in the case of the sample spun at  $2250 \text{ m min}^{-1}$ . The density and the X-ray crystallinities also show a similar trend. However, all the samples spun at higher speeds show an increase in birefringence. The X-ray diffractograms of the as-spun PP yarns are shown in Figure 3; the PP yarn spun at  $750 \text{ m min}^{-1}$  shows the presence of some amount of the metastable pseudohexagonal modification, although the crystal structure is largely made up of the stabler  $\alpha$ -monoclinic form. Samples obtained at higher spinning speeds show the existence of a fully evolved  $\alpha$  crystal modification with negligible amount of the pseudohexagonal crystal form.

**Table IV** Data on Physical and Structural Characteristics of the As-Spun Samples

Sample	Throughput Rate (g/min)	Birefringence ( $\Delta n \times 10^3$ )	Density (g/cm <sup>3</sup> )	Density Crystallinity (%)	X-ray Crystallinity (%)
P750	14.75	10.5	1.3410	3.75	—
P1500	25.27	16.0	1.3438	7.33	—
P2250	31.87	30.0	1.3465	9.58	0.8
P3000	29.31	38.0	1.3480	10.83	2.2
N750	11.25	9.5	1.1319	33.48	9.1
N1500	23.04	18.0	1.1336	34.58	12.3
N2250	30.18	27.5	1.1321	33.61	13.3
N3000	34.56	30.0	1.1325	33.87	16.8
PP750	12.9	13.0	0.9061	56.6	42.9
PP1500	18.7	19.0	0.9141	65.3	52.1
PP2250	22.5	23.0	0.9109	61.84	50.0
PP3000	26.0	25.0	0.9157	67.0	48.2

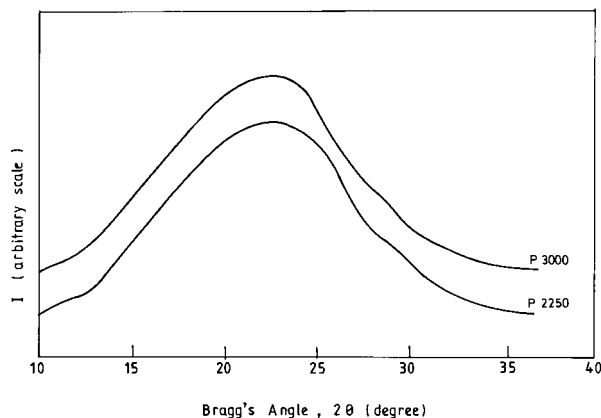
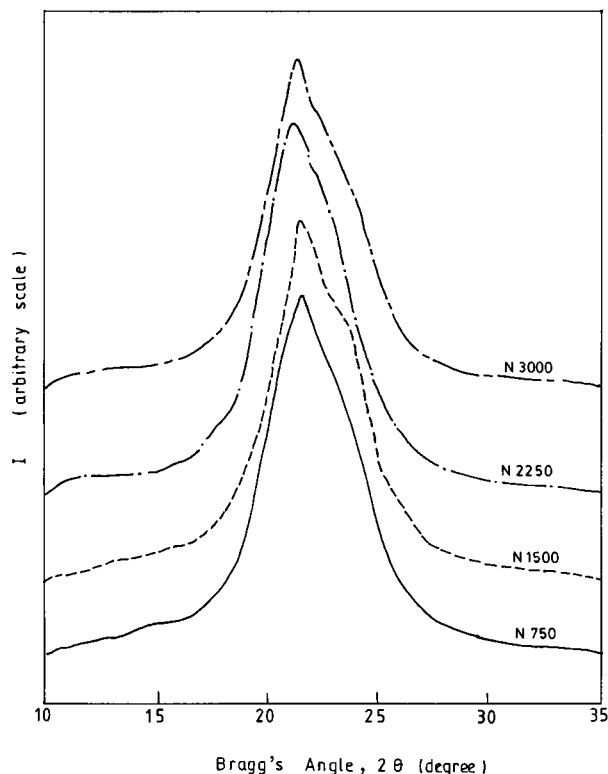
### Thermal Analysis of the As-Spun Yarns

The DSC heating thermograms for the as-spun yarns are reproduced in Figure 4 for PET, Figure 5 for N6, and Figure 6 for PP samples. The data extracted from these thermograms are summarized in Table V; some of the noteworthy observations are made below.

The glass transition temperature of the PET yarns (Table V) appears quite distinctly at  $\sim 78^\circ\text{C}$  and is apparently independent of the spinning speed. In the case of N6 and PP yarns, the glass transition temperatures, being low, do not show up in the thermograms (Figs. 5 and 6).

The cold crystallization exotherms are observed only with the as-spun PET yarns. This is an expected result since the PET fibers produced at spinning speeds of up to  $3000 \text{ m min}^{-1}$  are almost entirely amorphous, and hence crystallize

during the DSC thermal cycle. On the other hand, N6 and PP yarns are crystalline to a significant degree in the as-spun states and therefore do not show a distinct cold crystallization peak. The cold crystallization peaks observed with as-spun PET yarns show two noteworthy features. First, the samples produced at higher spinning speeds show a shift in the cold crystallization peak to lower

**Figure 1** I-2 $\theta$  plots for two as-spun PET yarns.**Figure 2** I-2 $\theta$  plots for the four as-spun N6 yarns.

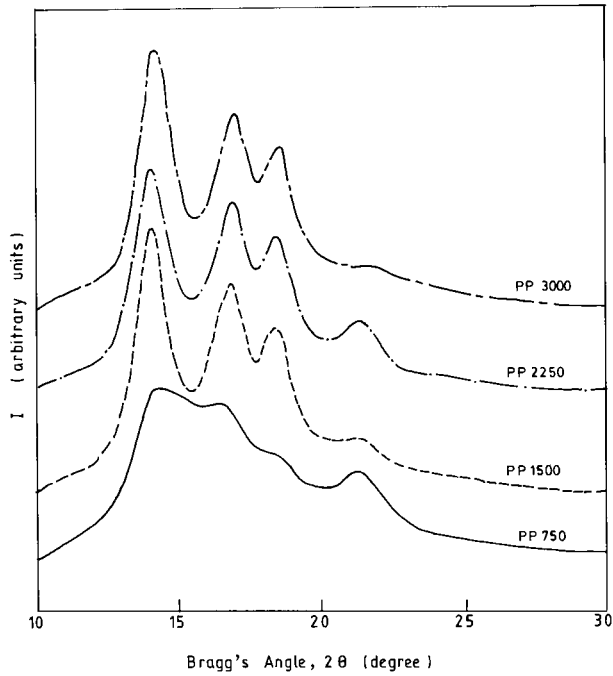


**Figure 3** I-2θ plots for the four as-spun PP yarns.

temperatures, apparently due to orientation, which allows orientation-induced crystallization to occur at lower temperatures. Second, the half-width of the cold crystallization peak is higher for the samples spun at higher spinning speeds due to their structure being less homogeneous.

In the case of PET, the peak temperature of the melting endotherm increases from 259°C for the yarn spun at 750 m min<sup>-1</sup> to 261°C for the

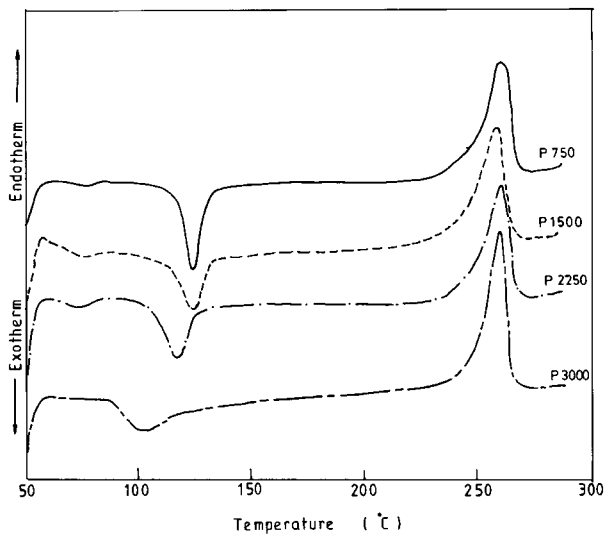


**Figure 4** DSC heating thermograms for the as-spun PET yarns.

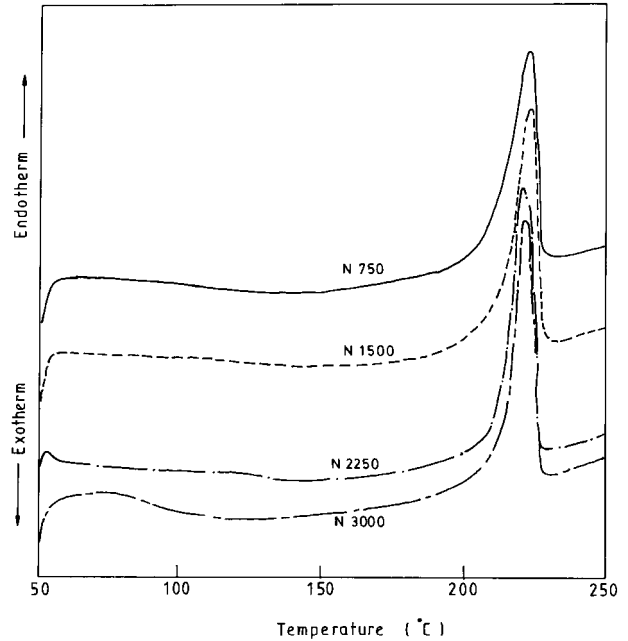


**Figure 5** DSC heating thermograms for the as-spun N6 yarns.

yarn spun at 3000 m min<sup>-1</sup>. On the other hand, the melting characteristics of N6 and PP as-spun yarns show hardly any dependence on the spinning speed.

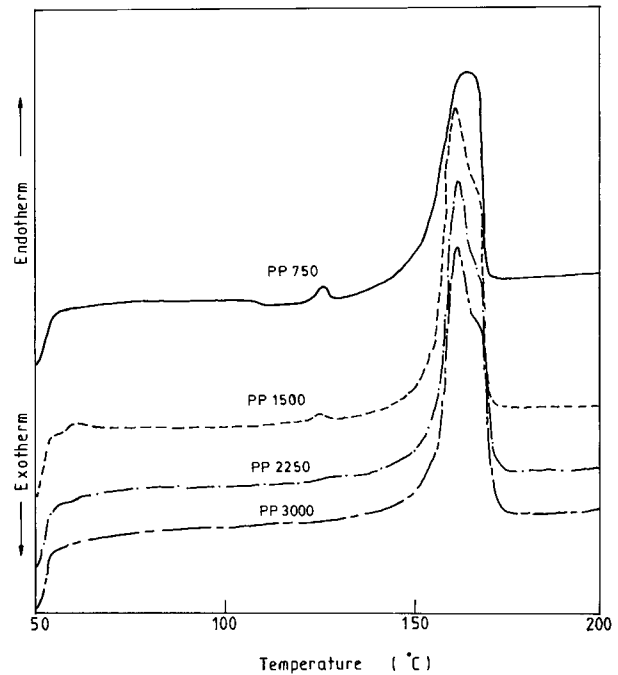


**Figure 6** DSC heating thermograms for the as-spun PP yarns.

**Table V** Data Extracted from DSC Thermograms

Sample	$T_g$ (°C)	$T_{CC}$ (°C)	$T_m$ (°C)	$T_c$ (°C)	$\Delta H_f$ (J/g <sup>-1</sup> )	DSC Crystallinity (%)
P750	79.2	125.0	259	213	20.16	14.6
P1500	77.7	123.0	258	215	33.9	24.5
P2250	77.8	117.0	260	214	25.0	18.1
P3000	—	105.0	261	217	35.6	25.8
N750	—	—	222	190	68.56	34.5
N1500	—	—	223	191	68.9	36.6
N2250	—	—	221	191	70.4	37.4
N3000	—	—	222	190	70.3	37.0
PP750	—	—	163.5	112	79.98	49.0
PP1500	—	—	162.5	113	89.66	55.0
PP2250	—	—	163.0	114	87.80	54.0
PP3000	—	—	163.0	115	83.30	51.0

The DSC heating thermograms of the as-spun PP yarns obtained at spinning speeds of 750 and 1500 m min<sup>-1</sup> show a small endotherm at ~ 130°C, its magnitude being very small for the yarn spun at 1500 m min<sup>-1</sup>. The origin of this endotherm may be traced to the following two events: (1) the transformation of the metastable pseudohexagonal crystal modification present in the as-spun yarns to the stabler  $\alpha$ -monoclinic crystal form. It is seen from the literature that the pseudo-hexagonal modification is unstable at temperatures > 110°C. The X-ray diffraction plots for these samples (Fig. 3) reveal that the yarns spun at 750 m min<sup>-1</sup> have a relatively higher content of the smectic modification. Samples spun at higher spinning speeds are not expected to contain any noticeable amount of the pseudohexagonal crystal form. (2) the melting of the  $\gamma$ -crystal modification, which incidentally melts at ~ 126°C. It is worth pointing out that the X-ray diffraction plots of these samples did not reveal any peaks associated with the  $\gamma$ -crystal modification.

The melting endotherms of the as-spun PP yarns show double peaks. Such doublets can arise either from the melting of that part of the material which recrystallizes during the DSC scan itself<sup>13</sup> and is called the recrystallizable fraction, or alternately, may be associated with the  $\beta$ -crystal phase, which also incidentally melts at a temperature of 170°C. However, it may be worth mentioning that the X-ray diffraction plots for these as-spun PP samples (Fig. 3) do not reveal any peaks associated with the  $\beta$ -crystal form, and it may be safely assumed that the doublet does not originate from their melting.

The DSC crystallinity values as estimated from the melting endotherms for all the as-spun yarns are listed in Table V. It may be seen that the PP yarns show the highest crystallinity and PET yarns the lowest with the N6 samples displaying intermediate values of crystallinity. It should be pointed out that the crystallinity, as obtained from the melting peaks, is not a measure of the initial crystallinity of the as-spun samples, but includes the effect on the sample of its thermal history during the DSC run.

The thermograms obtained during cooling are shown in Figure 7 for PET, Figure 8 for N6, and Figure 9 for PP, and the data extracted from the plots are presented in Table V. The peak temperature of crystallization during cooling for the as-spun PET yarns increases from 213°C for the 750 m min<sup>-1</sup> sample to 217°C for the 3000 m min<sup>-1</sup> sample. On the other hand, as-spun PP shows a very small increase, while in the case of the as-spun N6 yarns there is no significant effect.

### Drawing Characteristics of As-Spun Yarns

An important requirement of the present investigation was to ensure that the throughput rate at any particular spinning speed was so chosen that when the as-spun multifilament yarn was drawn to an appropriate draw ratio, a fully drawn 60/52 multifilament yarn with breaking extension of ~ 30% was obtained. In the case of N6 and PP, the first set of samples did not yield drawn samples of the required characteristics. Hence, adjustments were made in the throughput rates, keeping all other spinning conditions unchanged and a fresh

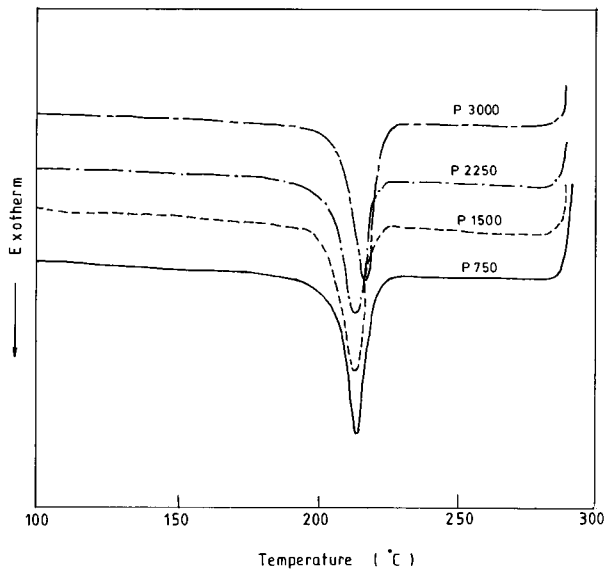


**Figure 7** DSC cooling thermograms for the as-spun PET yarns.

set of as-spun yarns was obtained which met the above requirements. The discussion that follows relates to the final set of as-spun yarns.

**Stress-Strain Characteristics of the As-Spun Yarns**

The stress-strain curves for the three sets of as-spun samples are shown in Figures 10-12 for

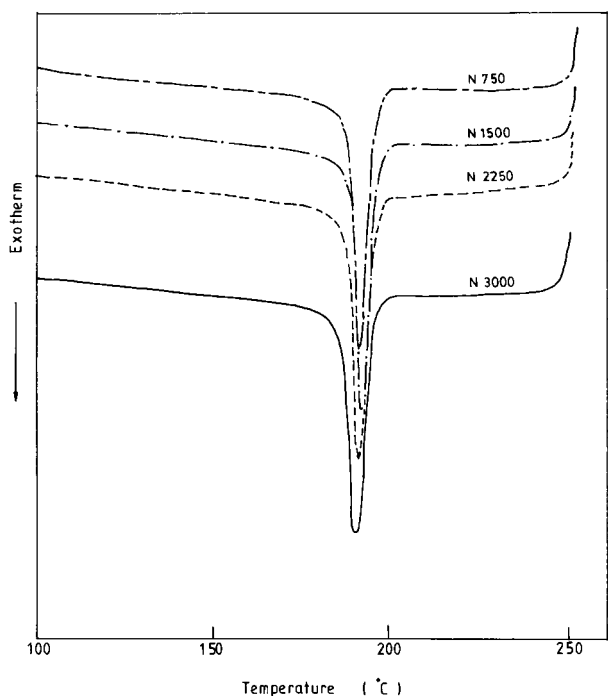


**Figure 8** DSC cooling thermograms for the as-spun N6 yarns.

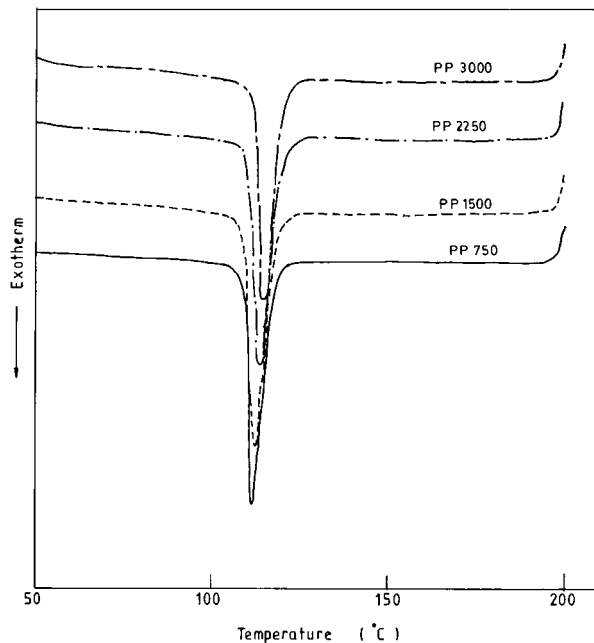


**Figure 9** DSC cooling thermograms for the as-spun PP yarns.

PET, N6, and PP, respectively. It can be seen from Figure 10 that all the as-spun PET samples show a distinct yield point with necking. The yield stress is higher in the samples spun at higher spinning speeds and is also accompanied with a progressive reduction in the natural draw ratio. This type of behavior is expected from a rubberlike network. In the case of N6 (Fig. 11) and PP (Fig. 12), the second set of samples have been studied for their stress-strain behavior. Unlike PET, the stress-strain curves of the as-spun N6 fibers (Fig. 11) do not show necking but do show a distinct yield point followed by strain hardening.

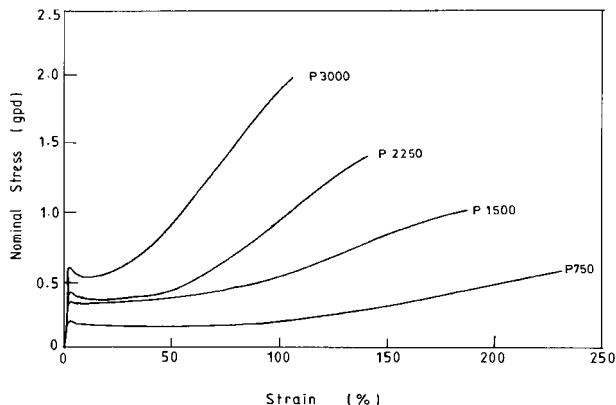


**Figure 10** Stress-strain curves for the as-spun PET yarns.

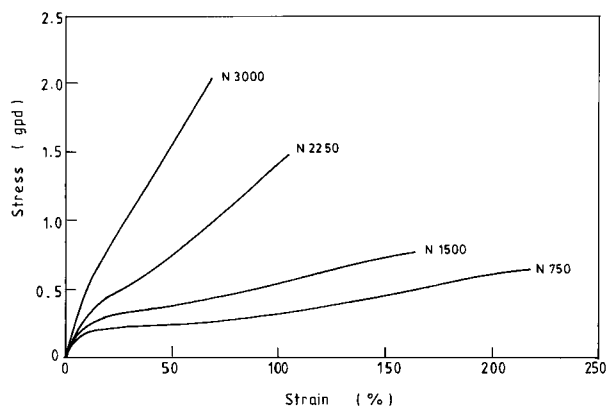


**Figure 11** Stress-strain curves for the as-spun N6 yarns.

The absence of necking during yield may be attributed to the lowering of the glass transition temperature of N6 by moisture to a temperature below the temperature at which tensile testing was conducted (20°C). In the case of the as-spun PP yarns also, a distinct but neck-free yield point may be observed (Fig. 12), and it is followed by a pronounced strain hardening effect.

The tenacity, modulus, and breaking elongation of the three sets of as-spun yarns show the expected behavior (Table VI); with increase in spinning speed, the tenacity and modulus increase while the extension-to-break decreases. The residual draw ratio for the three sets of as-spun samples is plotted in Figure 13 as a function of spinning speed; the drop of residual extensibility is most steep for the N6 samples followed by that for PET, while the curve is rather flat for the PP sample.

#### The Effect of Spinning Speed and Throughput Rate on Orientation and Drawability

Concurrent changes in throughput rate and take-up speed have a predominant effect on the orientation and structure developed in the as-spun yarns. This aspect is of particular interest, since increase in production is directly related to the residual extensibility of the as-spun yarns, which is in turn related to their orientation.

The birefringence data shown in Table IV are plotted as a function of spinning speed for all the three polymers in Figure 14, and shows two noteworthy features. First, in the case of PET, the birefringence rises rapidly in the range of spinning speeds investigated, while for PP the rate of increase is small, with N6 showing intermediate

behavior. Second, while PP and N6 develop a substantial part of the birefringence of the fully drawn yarn during spinning itself, in the case of PET that is not the case (Table VII). This is at least partly related to the noncrystalline nature of as-spun PET.

The above-mentioned differences in orientation and crystallinity follow largely from the intrinsic differences in response due to the characteristics of the individual polymer considered. The orientation developed during melt spinning of PET fibers is dependent on the stress developed during spinning.<sup>14,15</sup> In the as-spun N6 yarns, the initial orientation developed during spinning can also be expected to play a pivotal role in the development of crystallinity and other structural changes on the takeup bobbin after the winding is complete. The onset of crystallization in the spinline in the case of PP,<sup>16</sup> and with N6 at spinning speeds of 2000 m min<sup>-1</sup> and above, is also known to strongly depend on the stresses developed during spinning. Hence, the effect of simultaneous increase in spinning speed and throughput rate on the spinline stress during melt spinning of the three polymers is briefly discussed below in terms of the dynamics of the melt spinning process and the characteristic differences in their response resulting from their properties.

It is well known that increase in throughput rate lowers the spinline stress, while an increase in spinning speed increases it.<sup>15</sup> If the contributions match, then there would not be any significant effect of the simultaneous changes in throughput rate and spinning speed on the spun yarn characteristics. In the case of PET, sensitivity analysis<sup>15</sup> shows that increase in spinning speed has a greater effect on the spinline stress

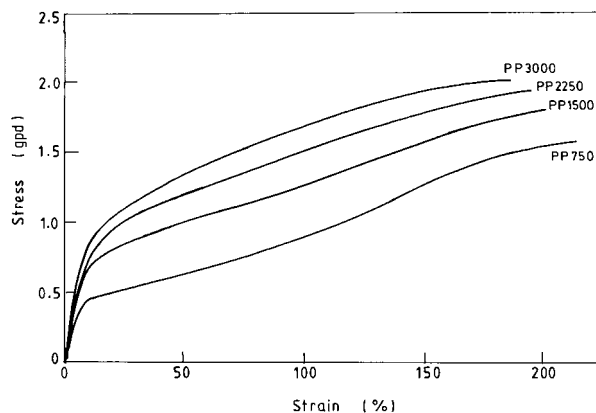


**Figure 12** Stress-strain curves for the as-spun PP yarns.

**Table VI Mechanical Properties of As-Spun Yarns**

Sample	Throughput Rate (g/min)	Breaking Elongation (%)	Tenacity (gpd)	Initial Modulus (gpd)	Natural Draw Ratio
P750	14.75	230	0.56	13.0	2.15
P1500	25.27	185	1.00	18.0	1.45
P2250	31.87	140	1.42	22.0	1.53
P3000	39.31	105	1.99	31.0	1.30
N750	14.97	212	0.94	3.5	—
N1500	24.20	148	1.47	5.5	—
N2250	26.50	100	2.08	8.0	—
N3000	28.80	73	2.50	10.5	—
PP750	13.6	212	1.57	4.0	—
PP1500	24.4	200	1.82	4.2	—
PP2250	34.6	196	1.97	4.4	—
PP3000	44.5	187	2.03	5.0	—

than a similar increase in throughput rate. This situation is largely due to increased contributions to the spinline stress from inertial and air drag effects, although viscoelastic effects arising due to increase in the rates of deformation at higher spinning speeds can also be expected to make a contribution to the increase in spinline stress. Similar observations also hold for N6<sup>17</sup> in the spinline, since most of the crystallization takes place on the bobbin during conditioning. However, in the case of PP, the spun fiber structure is dominated by the crystallinity and the crystal modification developed during melt spinning.<sup>16</sup> The effects of spinning speed and throughput rate on spinline stress, as discussed for PET and N6, continue to hold true even during spinning of PP yarns, at least in the region close to the spinneret where no crystallization takes place. Higher spinline stresses arising due to the use of higher spin-

ning speeds merely shift the temperature of onset of crystallization to higher temperatures. The onset of crystallization also results in a large increase in the viscosity of the polymer and ensures minimal changes in the orientation following the onset of crystallization, in spite of an increase in spinline stress largely due to air drag effects. The inertial contribution after the crystallization is negligible since the filaments do not undergo any further acceleration. In essence, during melt spinning of N6 and PET, the response to stress in the spinline is akin to that of a rubberlike network, while in the case of PP, the response to stress does not resemble that of a rubberlike network due to the fact that the polymer undergoes substantial crystallization quite early in the spinline. Hence, an increase in spinline stress due to the use of higher spinning speeds does not generate a corresponding increase in orientation in the as-spun

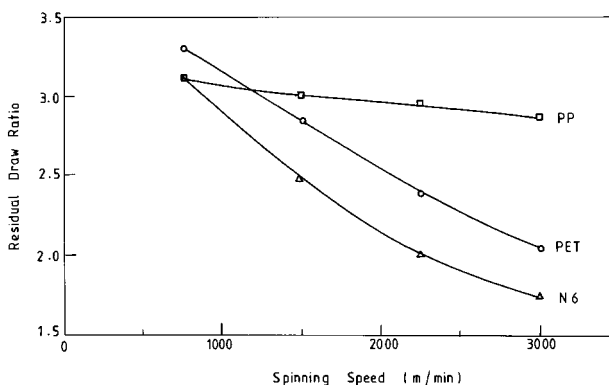


**Figure 13** Dependence of residual draw ratio on the spinning speed for the three polymers.

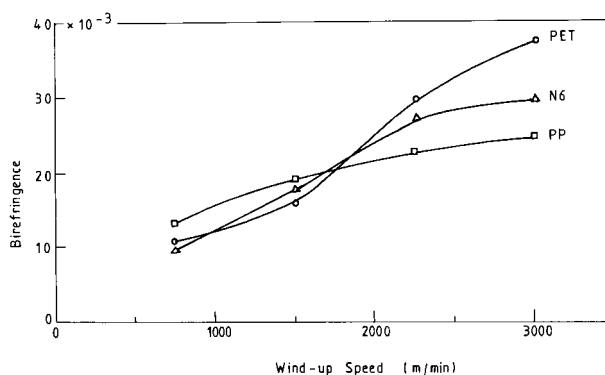


**Figure 14** Dependence of birefringence of the as-spun yarns on spinning speed.

**Table VII Structural Data for the Drawn Yarns**

Sample	Birefringence ( $\Delta n \times 10^3$ )	Density (g/cm <sup>3</sup> )	Density Crystallinity (%)
P750	153	1.3835	40.4
P1500	153	1.3845	41.2
P2250	153	1.3841	40.9
P3000	150	1.3842	41.0
N750	59	1.1573	49.8
N1500	58	1.1559	48.9
N2250	61	1.1580	50.3
N3000	60	1.1594	51.2
PP750	33.1	0.9136	64.8
PP1500	33.0	0.9152	66.5
PP2250	33.0	0.9150	66.3
PP3000	34.0	0.9154	66.7

PP yarns. Orientation and other structural differences in the yarns spun at different speeds are hence smaller in comparison to N6 and PET. Conditions similar to those in PP are operative during high-speed spinning of N6 fibers, especially at spinning speeds of 3000 m min<sup>-1</sup> and above. Stress-induced crystallization introduces features that are similar to those during melt spinning of PP, and hence offers an opportunity to use spinning speeds of 4000–4500 m min<sup>-1</sup> and improve production rates.

It has been pointed out<sup>18</sup> that in N6 and PET, the microfibrils, which form the basic unit of structure in the drawn state, form an endless interwoven structure like a network. Polypropylene yarn in the undrawn state is relatively highly

crystalline and the crystallites are believed to be in the form of lamellae. Since the crystallinities of the various as-spun PP samples are not very different, their extensibilities are also not very different from each other. It has been stated<sup>19</sup> that the deformation and rearrangement of the morphological structure in spun PP fibers occurs through shear, tilt, rotation, and separation of the lamellae; with sufficient deformation, the lamellae are broken up into folded chain blocks  $\sim 200$  Å in width. These blocks subsequently aggregate to form the basic unit of the drawn fiber, i.e., the microfibril.

It has been pointed out to us by the referee that an additional/alternative cause for the low elongation-at-break of highly oriented N6 and

**Table VIII Mechanical Properties of Drawn Yarns**

Sample	Breaking Elongation (% at room temp)	Tenacity (gpd)	Initial Modulus (gpd)
P750	18.50	3.25	61
P1500	21.80	3.34	67
P2250	20.39	3.45	68
P3000	22.44	3.50	73
N750	21.35	2.45	27
N1500	24.50	2.53	25
N2250	33.20	2.56	20
N3000	18.02	2.75	23
PP750	26.88	5.33	33
PP1500	24.32	5.33	29
PP2250	27.89	4.80	32
PP3000	26.95	4.90	34

**Table IX** Throughput Rate and Related Data

Sample	Throughput Rate (g min <sup>-1</sup> )	Spun-Yarn Denier	Residual Draw Ratio	Actual Draw Ratio	Drawn Yarn Denier	Reference Drawn Denier	Calculated Throughput Rate (g min <sup>-1</sup> )
P750	14.75	162.0	3.30	3.0	56.40	60	15.00
P1500	25.27	143.0	2.85	2.55	60.66	60	25.50
P2250	31.87	125.0	2.40	2.1	61.99	60	31.50
P3000	39.31	104.0	2.05	1.75	63.63	60	35.00
N750	14.97	179.0	3.12	2.85	63.05	60	14.25
N1500	24.20	142.0	2.48	2.18	66.58	60	21.80
N2250	26.50	105.5	2.00	1.70	62.35	60	25.50
N3000	28.80	84.5	1.73	1.43	60.40	60	28.60
PP750	13.60	162	3.12	2.80	58.00	60	14.00
PP1500	24.40	142	3.00	2.70	52.50	60	27.00
PP2250	34.60	134	2.96	2.65	51.00	60	39.75
PP3000	44.50	130	2.87	2.55	51.00	60	51.00

PET fibers spun at 3000 m/min could be the lower weight average molecule weight values of these condensation polymers. This is a valid suggestion. It is worth emphasizing at this stage that, as shown later in this article, the nature of the throughput versus spinning speed relationship for fibers of different molecular weights and processed under conditions quite different from ours show identical trends in as far as the enhancement of throughput rate with increase in spinning speed is concerned.

### Structure and Properties of Drawn Yarns

Drawn samples were obtained from the as-spun yarns using the residual draw ratio data presented in Figure 13. The drawing conditions used to obtain the first set of drawn yarns are given in Table II and are quite close to the conditions used to obtain the final set of drawn yarns.

The structural and mechanical characteristics of the drawn yarns are tabulated in Tables VII and VIII, respectively. Within a particular set of samples, the density, birefringence, and crystallinity computed using the density values can be seen (Table VII) to be within a rather narrow range. Comparison of the mechanical properties (Table VIII) like tenacity, breaking extension, and modulus obtained by carrying out tensile testing on an Instron tensile testing machine at room temperature, also showed a similar trend.

### Throughput Rate Characteristics

To achieve a fiber of constant drawn denier at different wind-up speeds, the throughput rate needs to be increased at higher wind-up speeds, depending on the residual draw remaining in the as-spun samples, which can be estimated using the procedure outlined earlier. Assuming the residual draw ratio to be independent of the throughput rate for any particular spinning speed, the throughput rate that would be required to obtain a drawn sample of the required denier can be computed by using eq. (1). It must be stated here that this assumption introduces a degree of approximation in the present approach.

Table IX lists the throughput rates used to obtain the final sets of as-spun yarns for PET, N6, and PP; in addition, the spun yarn denier, residual draw ratio of the as-spun yarns, actual draw ratio to which the yarn was subjected, the drawn and reference yarn denier, and the throughput rate calculated using eq. (1) to obtain a drawn yarn of a reference denier of 60 are also given. It is worth mentioning that the calculated throughput rate is quite close to the experimentally obtained throughput rate, thus justifying the use of eq. (1) to obtain an approximate estimate of the throughput rate.

The throughput rates for PET as function of wind-up speed are plotted in Figure 15. The plot also shows data obtained by various researchers,<sup>4,20,21</sup> as obtained by back calculations from their load elongation data. Two points need to be

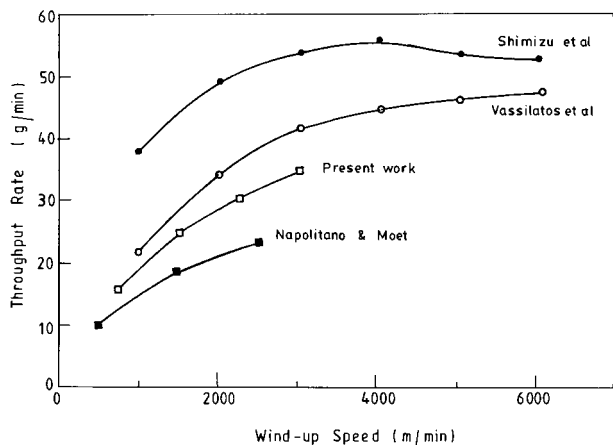


**Figure 15** Throughput rates used to obtain a drawn 60/52 multifilament yarn plotted as a function of wind-up speed for PET.

made at this stage. First, the estimate of throughput rate using back calculations from the load elongation data needs some explanation, which is attempted below. From the breaking elongation, which could be read off from the load elongation curve, the approximate residual draw ratio could be estimated, and hence the spun denier found. Then with the help of eq. (1), the mass throughput rate could be calculated. Secondly, it needs to be emphasized that the data of Shimizu, Okui, and Kikutani<sup>4</sup> used in the comparison in Figure 15 and subsequently in other figures were obtained with constant throughput rate. This imposes a limitation on its use as a result of the approximations used in the derivation of eq. (1), but since these are quite reasonable, it will be expected that the limitations will not be too great. There are significant differences in the magnitude of the throughput rates for a constant drawn denier of 60, although it may be seen that the general nature of the plots are all similar. It is possible to explain such differences on the basis of the molecular weight and the process variables used during spinning. Vassilatos, Knox, and Frankfort<sup>21</sup> report elongation-to-break data which are slightly higher than our results. This could be due to the use of higher spinning temperature, ranging from 295 to 310°C with increase in spinning speed, as against a constant spinning temperature of 290°C used in the present investigation. Napolitano and Moet<sup>20</sup> obtain lower extension-to-break values in comparison to our data. This can be attributed to the higher molecular weight used by them (number average molecular weight of 42,000) which results in higher stress during

spinning. Shimizu, Okui, and Kikutani<sup>4</sup> used throughput rates per spinneret hole which are at least 10 times higher than those used in the present study for PET. This can explain the much higher percentage extension-to-break observed in their samples.

In the case of N6, the plots of throughput rates required to obtain a drawn fiber denier of 60 at different spinning speeds are given in Figure 16. It can be seen that like PET, the throughput rates used by Shimizu, Okui, and Kikutani<sup>4</sup> are much higher than those used in the present study for N6 also. The nature of the plot obtained is, however, quite similar to that obtained for the present investigation.

In the case of PP, the plots of throughput rates required to obtain the drawn fiber denier of 60 at different spinning speeds obtained from the present studies and from the data of Shimizu, Toriumi, and Imai<sup>22</sup> and Fourne,<sup>23</sup> are shown in Figure 17. Again the throughput rates used by Shimizu, Toriumi, and Imai<sup>22</sup> are much higher, while those by Fourne<sup>23</sup> are close to those used in the present study. The plots are quite similar and show that in PP the gain in productivity with increase of spinning speed is substantial.

#### Comparison of the Throughput Characteristics for the Three Polymers

The throughput rate versus spinning speed plots for the three polymers studied are given in Figure

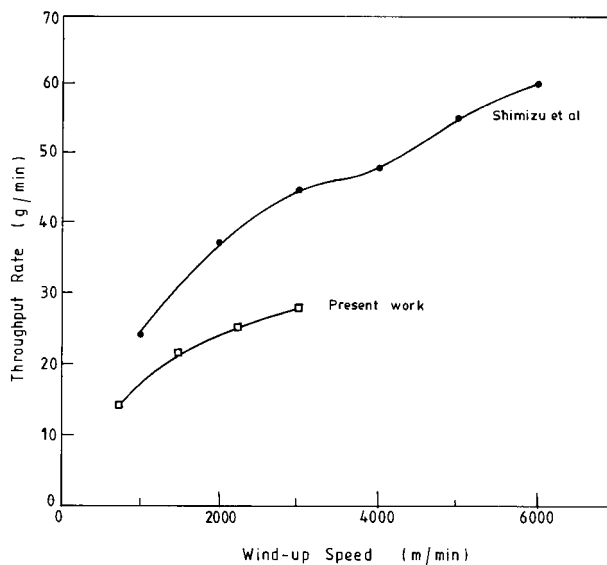


**Figure 16** Throughput rates used to obtain a drawn 60/52 multifilament yarn plotted as a function of wind-up speed for N6.

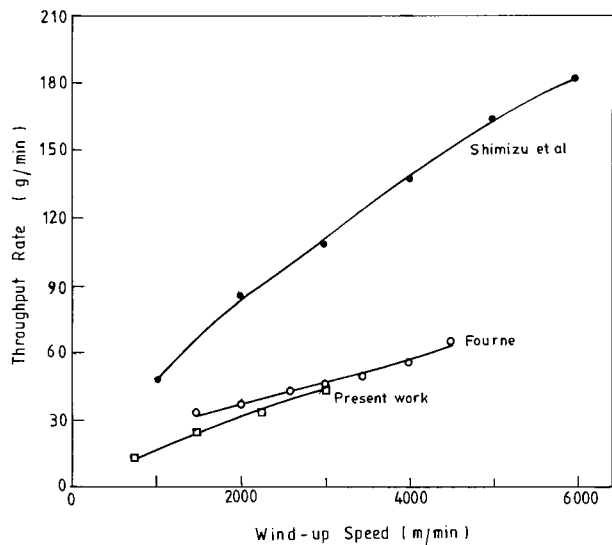


**Figure 17** Throughput rates used to obtain a drawn 60/52 multifilament yarn plotted as a function of wind-up speed for PP.

18(a); the corresponding plots from the work of Shimizu, Okui, and Kikutani<sup>4</sup> and Shimizu, Toriumi, and Imai<sup>22</sup> are shown in Figure 18(b). It may be observed that the throughput rate does not increase in the same proportion as the wind-up speed, and shows a saturation for N6 and PET at a wind-up speed of  $\sim 3000$  m min<sup>-1</sup>. However, for N6 it is clear from the data of Shimizu et al. that the throughput rate can be increased at spinning speeds  $> 4000$  m min<sup>-1</sup>. In the case of PP, there is almost a linear relationship between throughput rate and spinning speed. The change in the residual draw ratio of PP with increase in spinning speed is relatively much less than for the other two polymers, which is also reflected in the development of birefringence with spinning speed (Fig. 14). Due to the smaller increase in birefringence with increase in spinning speed, it is possible to use draw ratios which are very close to each other in samples spun at different speeds.

In the case of PET, the birefringence is sigmoidal in shape (Fig. 14) and begins to increase at a quicker rate at higher spinning speeds. Hence, at speeds  $> 3000$  m min<sup>-1</sup>, there is only a limited gain in throughput rate. In fact, according to the data of Shimizu et al. there may be a drop in the throughput rate requirement to obtain a drawn fiber denier of 60.

The birefringence versus spinning speed plots for the three polymers (Fig. 14), particularly the

difference between them, can be explained as follows. As stated earlier, PET and N6 do not show significant crystallization in the spinline, and thus can be considered to form rubberlike networks; thus they show a higher degree of orientation at higher spinning speeds. N6 becomes closer in response to PP at speeds of  $4000$  m min<sup>-1</sup> or above, as it crystallizes in the spinline and hence offers scope for improvement in productivity by increase in spinning speed.

It is obvious that the scope for improvement in throughput with spinning speed is most pronounced in the case of PP, due to its higher crystallizability and relatively low rate of development of orientation in the as-spun yarns with increase in spinning speed.

## CONCLUSIONS

Throughput rate does not rise in proportion to the spinning speed in all the three polymers studied.

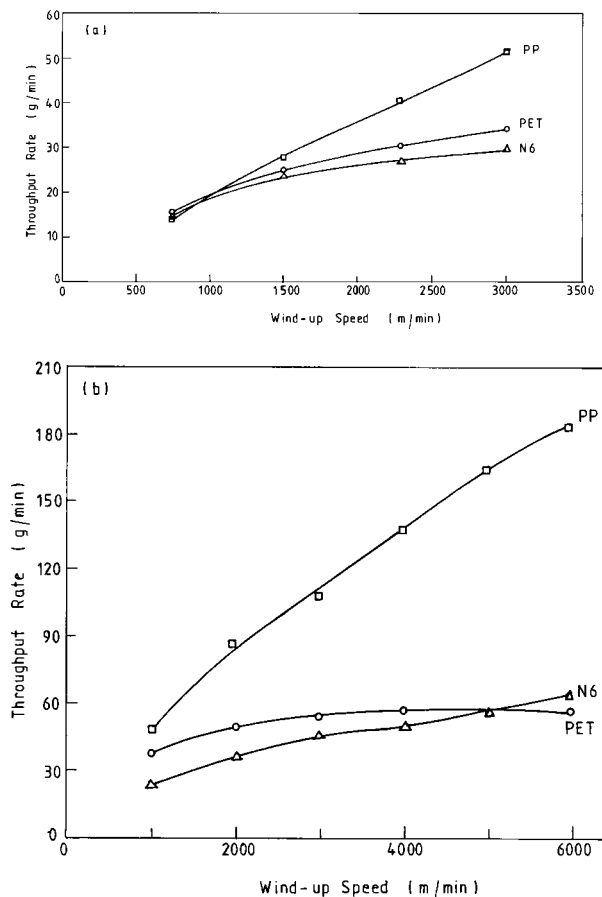


**Figure 18** Comparison of the dependence of throughput rate on wind-up speed for the three polymers. (a) Present data, (b) Shimizu et al.'s data.

Increase in the spinning speed leads to improvement of molecular orientation, which is reflected in the birefringence values and a consequent reduction in the residual draw ratio. The birefringence profiles as a function of spinning speed show significant differences and have important implications on the enhancement of productivity during spinning. These differences in the development of orientation are related to the polymer characteristics and its behavior in the spinline. It was found that the birefringence development with spinning speed in the PP samples is relatively less than in the other two polymers. This has been attributed to the higher crystallizability of PP and the use of higher spinning speeds only increases the temperature of onset of crystallization in the spinline and does not impart significant changes in the overall structure developed by melt spinning. The gain in productivity with increase in spinning speed is maximum for PP. The present study suggests that if development of orientation in the spinline can be suppressed, productivity will increase.

The authors are grateful to the referee for his very perceptive comments on the manuscript.

## REFERENCES

1. K. Riggert, *Modern Textiles*, Alfred H. McCollough, Rayon Publishing Corporation, New York, July, 1974, p. 63.
2. H. M. Heuvel and R. Huisman, in *High Speed Melt Spinning*, A. Ziabicki and H. Kawai, Eds., Wiley, New York, 1985.
3. E. H. Boasson and K. Makishima, *J. Polym. Sci.*, **17**, 311 (1955).
4. J. Shimizu, N. Okui, and T. Kikutani, in *High Speed Melt Spinning*, A. Ziabicki and H. Kawai, Eds., Wiley, New York, 1985.
5. H. M. Heuvel and R. Huisman, *J. Appl. Polym. Sci.*, **22**, 2229 (1978).
6. R. P. Daubney, C. W. Bunn, and C. J. Brown, *Proc. Roy. Soc. (A)*, **226**, 531 (1954).
7. J. Brandrup and E. H. Immergut, Eds., *Polymer Handbook*, Wiley, New York, 1975.
8. B. Wunderlich, *Macromolecular Physics*, Vol. I, Academic Press, New York, 1976.
9. G. Farrow and D. Preston, *Brit. J. Appl. Phys.*, **11**, 353 (1960).
10. G. Farrow, *Polymer*, **1**, 520 (1961).
11. D. R. Holmes, C. W. Bunn, and D. J. Smith, *J. Polym. Sci.*, **17**, 159 (1955).
12. H. Arimoto, *J. Polym. Sci., Ser. A*, **1**, 2283 (1964).
13. V. B. Gupta, C. Ramesh, and A. K. Gupta, *J. Appl. Polym. Sci.*, **29**, 3727 (1984).
14. A. Ziabicki and K. Kedzierska, *J. Appl. Polym. Sci.*, **2**, 111 (1962).
15. Y. C. Bhuvanesh and V. B. Gupta, *Indian J. Text. & Fibre Res.*, **15**, 145 (1990).
16. Y. C. Bhuvanesh and V. B. Gupta, *J. Appl. Polym. Sci.*, **58**, 663 (1995).
17. K. F. Ziemiński and J. E. Spruiell, *J. Appl. Polym. Sci.*, **35**, 2223 (1988).
18. D. C. Prevorsek and H. J. Oswald, in *Solid State Behaviour of Linear Polyesters and Polyamides*, J. M. Schultz and S. Fakirov, Eds., Prentice-Hall, New Jersey, 1990.
19. M. Wishman and G. E. Hagler, in *Handbook of Fibre Science and Technology*, Vol. IV, M. Lewin and E. M. Pearce, Eds., Marcel Dekker Inc., New York, 1985.
20. M. J. Napolitano and A. Moet, *J. Appl. Polym. Sci.*, **32**, 4989 (1986).
21. G. Vassilatos, B. H. Knox, and H. R. E. Frankfort, in *High Speed Melt Spinning*, A. Ziabicki and H. Kawai, Eds., Wiley, New York, 1985.
22. J. Shimizu, K. Toriumi, and Y. Imai, *Sen-i-Gakkaishi*, **33**, 1977, T-255 as quoted in Ref. 15.
23. F. Fourne, *Man-Made Fibre Year Book*, Chemiefasern & Textilindustrie, Frankfurt, 1994, pp. 26-33.